

## CHAPTER 7

# *The Tropospheric Circulation Over Africa and its Relation to the Global Tropospheric Circulation*

R. E. NEWELL and J. W. KIDSON

### ABSTRACT

Long-term monthly mean zonal and meridional winds over Africa are presented for levels between 1000 and 100 mb in the form of maps and cross-sections. Desert dust transport depends on these winds in three ways: the winds control the flux and convergence of moisture which in turn governs the rainfall and hence the availability of dust at the surface; the surface wind strength regulates the pick-up of dust; the mean flow pattern controls the path of dust after it leaves the source.

We attempt to explain the classical Arrhenius–Turekian haze maps in terms of these three inter-relationships. Latitude–time sections of the monthly mean 850 mb zonal wind and rainfall along the prime meridian and along 40°E show the most favourable latitudes and months for dust transport. Along the meridian 10–15°N in January, 25–30°N in July and 25°S throughout the year are the most favoured regions for westward transport (see Figure 6a). At 40°E eastward transport occurs in June–August in the 5–30°N latitude band and over much of the year at 30–35°S. Rainfall amounts along the prime meridian of less than 1 cm per month are shown shaded in the Figure. The difference in character of the dust (red-brown in summer, grey to black in winter) emerges clearly from these sections which show a Saharan summer source and a Sahelian winter source.

The interhemispheric monsoon northerly flow examined in detail by Findlater is very strong near 40°E in the April–October period at 850 mb, with a return flow in the upper troposphere.

The mean flow data may be used directly for dust transport calculations, with air concentration data, as it seems likely that eddy flux contributions are small as has been found for water vapour. Such computations need base maps of soil state *vs.* season.

Examples of flow differences between a wet period, 1958–1962, and a dry period, 1970–1973, are given. It has been shown elsewhere (Kidson, 1977) that the 850 mb trough in the Sahelian region is more marked and the 200 mb flow is stronger in wet than in dry years. Here we try to assess the influence of these changes on dust transport patterns. It seems evident that dust in Atlantic deep-sea cores is governed both by the rainfall and the wind patterns: a change in the seasonal excursion of the Hadley cell in ice ages, for example, could influence the observed core concentrations as much as a change in wind strength.

The time variations of the mean winds over the past 25 years are thought to be related to global circulation pattern changes. Some aspects of these possible changes are illustrated using tropospheric temperature data and sea surface temperature data from the Pacific, Atlantic and Indian oceans. Data on a much longer time scale have also been examined and it is concluded that the exact physical cause of changes in flow over Africa has not yet been isolated.

## 7.1 INTRODUCTION

The tropospheric circulation influences the transport of African desert dust in three ways: the winds control the flux and convergence of moisture which in turn governs the rainfall and hence the availability of dust at the surface together with the washout; the surface wind strength regulates the pick-up of dust; the mean flow pattern controls the path of dust after it leaves the source. In this paper the long-term mean characteristics of the tropospheric circulation and rainfall are discussed. Changes in the tropospheric circulation over Africa are related to changes in the global atmospheric circulation and hypotheses to explain the changes are put forward.

The classical books by Kendrew (1961) and Griffiths (1972) give a detailed summary of the surface climatology of each country and the Atlas of Thompson (1965) covers much of the free-air climatology as well as rainfall by a beautiful set of maps. The climate of the Sahara has been thoroughly discussed by Dubief (1959, 1963). Prior work at M.I.T. (Newell *et al.*, 1972) provided seasonal maps of the wind components at levels between 1000 mb and 100 mb together with maps of vertical motion deduced from the continuity equation (Newell *et al.*, 1974). Another source of flow pattern information, which contains examples of daily patterns, is the Munitalp Foundation Symposium on Tropical Meteorology in Africa (1960). Considerable fundamental work on the flow patterns has also been carried out by Flohn and his colleagues (e.g. Flohn, 1965; Flohn and Korff, 1965; Struning and Flohn, 1969).

The main phenomenon which characterizes the tropospheric circulation is the intertropical convergence zone (ITCZ) and its steady seasonal migration. The cloudiness and rainfall associated with this phenomenon move to the south in northern winter and to the north in northern summer, reaching their extreme northerly position over the Sahel in August. The main features of this zone appear in the surface streamline and pressure patterns of Griffiths and Soliman (1972) and the surface flow is discussed in this volume by Dubief (1979). The ITCZ runs west-east across Africa until at about 25°E it turns southwards in winter and becomes indistinguishable from the surface boundary between the Atlantic Ocean westerlies and the Indian Ocean easterlies. In summer the ITCZ continues eastwards to the Persian Gulf. To the north and south of the ITCZ there are regions of large scale subsidence with the largest region north of the equator in winter being associated with the extreme southern excursion of the rising motion. The zonally averaged mass flux patterns shown in Figures 7.1 and 7.2 illustrate the subsidence

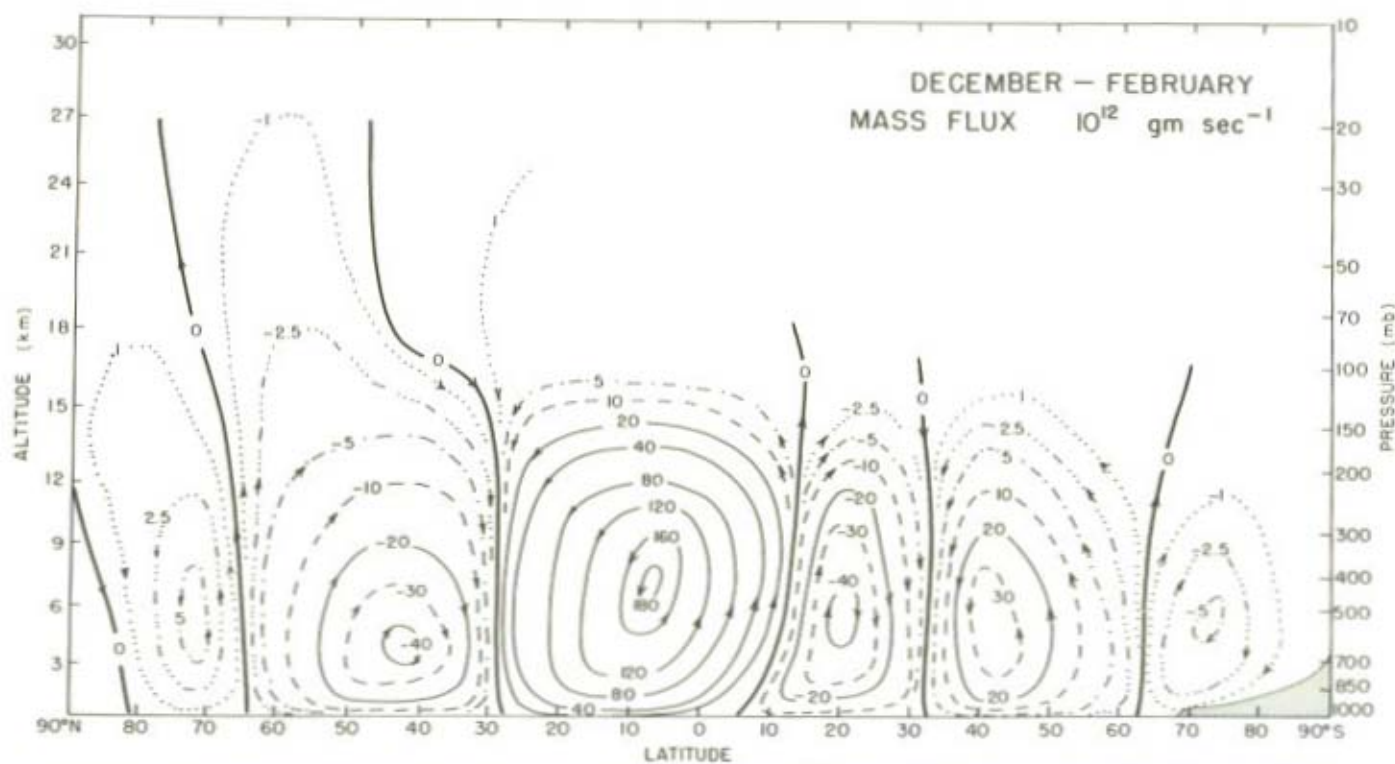


Figure 7.1 Zonally averaged mass flux December-February. Units:  $10^{12} \text{ gm sec}^{-1}$  (Redrawn from Newell *et al.*, 1972)

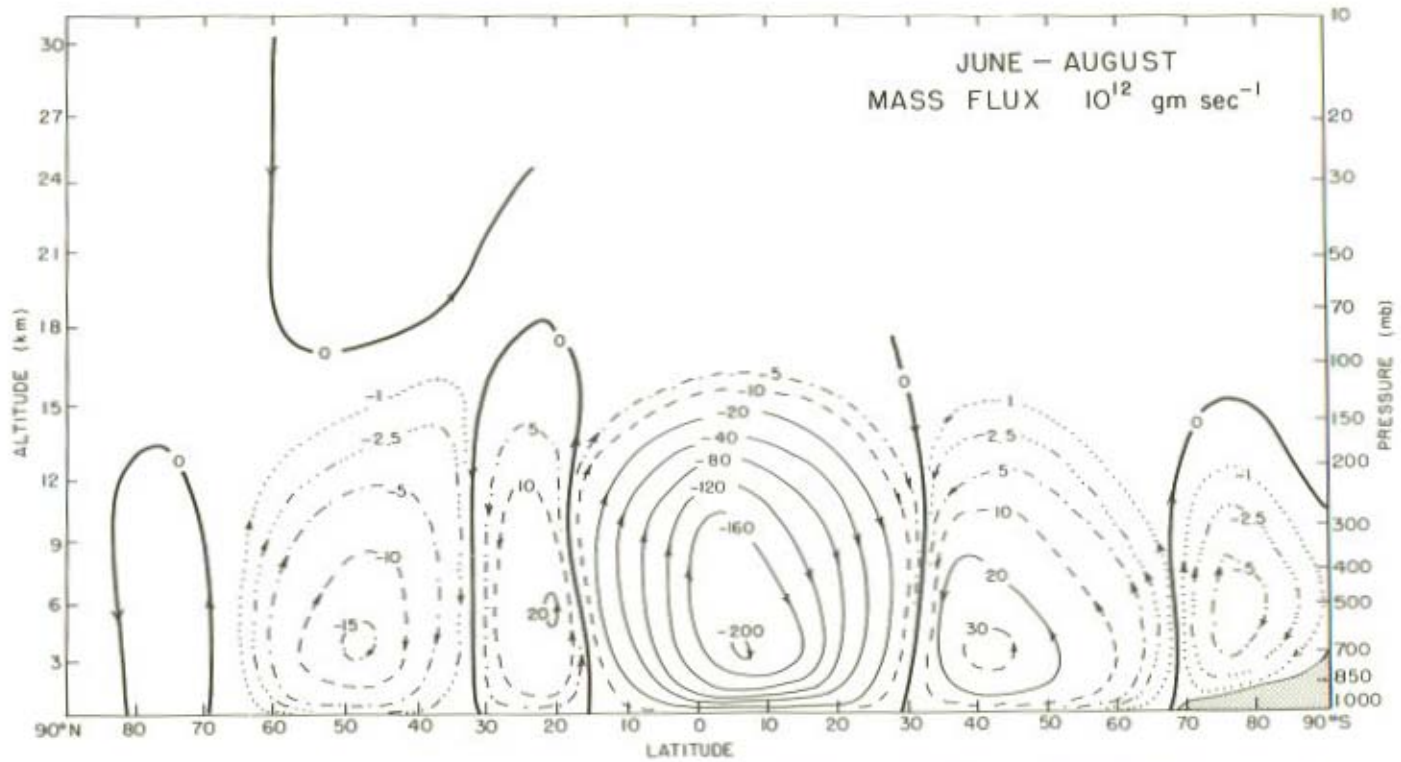


Figure 7.2 Zonally averaged mass flux June-August. Units:  $10^{12} \text{ gm sec}^{-1}$  (Redrawn from Newell *et al.*, 1972)

regions and it is, of course, this aspect of the global circulation which is responsible for the occurrence of deserts. At the northern and southern extremities of the continent the phenomena which characterize the circulation are the middle latitude baroclinic zones and the associated low-pressure rain-bearing transient systems, these being closest to the equator in the winter of the appropriate season. The description by means of the boundary layer climatology cannot be extrapolated upwards and there are, in fact, strong longitudinal variations in the upper troposphere which are significant in the dust transport problem.

## 7.2 LONG-TERM MEAN PATTERNS

### 7.2.1 Wind velocity

As part of a recent study of African rainfall and possible causes of Sahelian drought (Kidson, 1977) mean winds, moisture, and rainfall records have been assembled for all available African stations. Rainfall data cover the period 1951–73 (some of these were collected as part of the previous study of this problem by Tanaka *et al.*, 1975). Wind and moisture data covered the two periods, May 1958 to April 1963 and December 1969 to December 1973, data for the latter being obtained from the monthly Climatic Data for the World upper air tape. Upper air stations used are those shown in Figure 7.3. Rainfall stations are essentially the same as those shown in the map by Tanaka *et al.* (1975). Long-term mean monthly wind components have been plotted by computer on maps at levels between 1000 mb and 100 mb and the Cressman (1959) analysis procedure has been used to obtain an objective analysis on a  $5^\circ$  grid covering the region  $33^\circ\text{N}$  to  $33^\circ\text{S}$  and  $15^\circ\text{W}$  to  $45^\circ\text{E}$ . It was found necessary to use an anisotropic scan radius for the zonal wind component above the surface. While the meridional component is representative of a  $5^\circ$  grid square, the zonal component is representative of a  $15^\circ$  longitude,  $5^\circ$  latitude grid region. The components rather than streamlines are selected for illustration here as these values may be used directly in dust transport computations.

Examples of the analysed maps for 850 mb and 200 mb for four mid-season months are shown in Figures 7.4, 7.5, 7.6 and 7.7. The 850 mb zonal component, henceforth denoted by  $u$ , exhibits mainly variation with latitude in January, with easterly 'jets' at  $10^\circ\text{N}$  and  $20^\circ\text{S}$  and westerly flow north of  $25^\circ\text{N}$ , south of  $30^\circ\text{S}$  and in the  $0$ – $15^\circ\text{S}$  zone. Maximum values occur to the north and to the south of the Sahara. In July there are substantial variations with longitude with a reversal from easterly to westerly winds across the Sahara. Maximum values occur at about  $25^\circ\text{N}$  near the prime meridian and at about  $15^\circ\text{S}$ . Flow from the west dominates the equatorial zone and both regions of easterlies are further north than in January. The  $15^\circ$  longitude scan radius should be borne in mind whenever appreciable longitudinal variations appear in the actual data. In July, for example, the westerlies



The patterns at other levels may be viewed from a similar set of maps, but the portrayal of the vertical coherence cross-sections of the components is shown in Figures 7.8 and 7.9. The prime meridian is included, even though data is absent in the Southern Hemisphere, because it is representative of the western Sahara. The figures capture the essence of the basic mechanics namely that the Coriolis torque, acting on the meridional flow, governs the zonal wind field. Polewards motion in both hemispheres gives rise to westerly winds, as is very evident in the upper troposphere; likewise equatorwards flow is associated with easterly winds. The patterns of the zonal wind maps of Figures 7.4 to 7.7 can also be accounted for with this principle. The sections also show that poleward flow in the upper troposphere is accompanied by equatorward flow in the lower troposphere. Figure 7.10 is a cross-section along the equator and beside longitudinal variations this also illustrates the compensation between the upper and lower troposphere.

It seems necessary to consider variations on a month-to-month basis for the dust transport problem and Figures 7.11, 7.12, 7.13, and 7.14 show values of  $u$  and  $v$  at three longitudes for 850 mb and two longitudes for 200 mb. The main interest here is the Sahara and it is recognized that data is poor south of the equator for  $0^\circ$  longitude. The problem is not so serious for the  $u$ -component as for the  $v$ -component because of the anisotropic influence radius. In the western Sahara strongest easterly winds at 850 mb occur at  $10\text{--}15^\circ\text{N}$  in the winter and at  $25^\circ\text{N}$  in the late summer. At  $40^\circ\text{E}$  there are westerlies from the equator northwards in the summer.

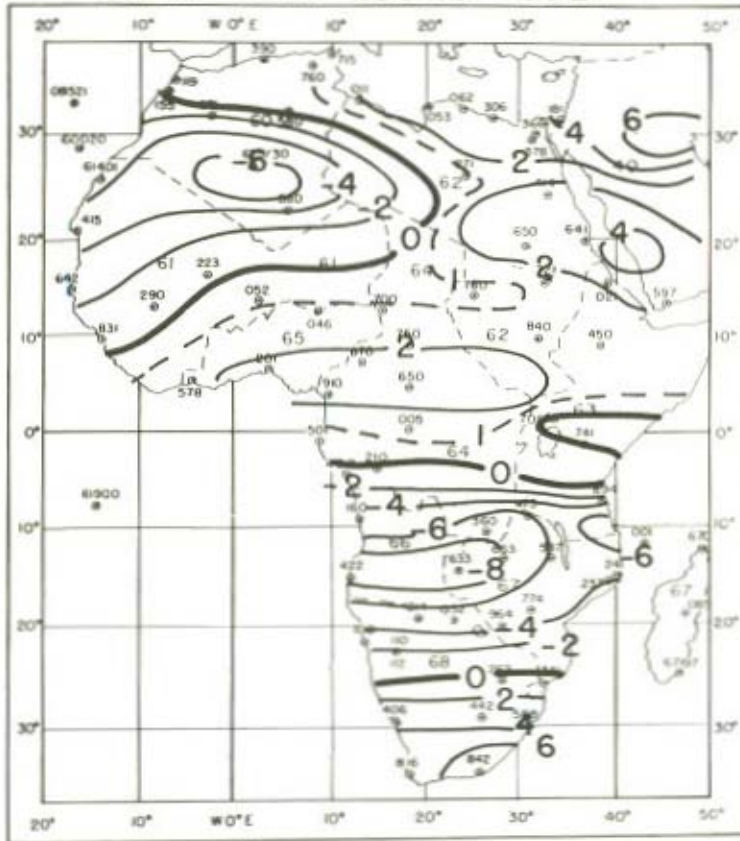
The strong flow at 850 mb from the southern to the northern hemisphere at  $40^\circ\text{E}$ ,  $5^\circ\text{S}$  in summer is worth noting. The low level jet in this region discovered by Findlater (1969a,b; 1972) is a little underestimated in strength by the analysis technique; in fact, Findlater reports a mean of  $15\text{ m sec}^{-1}$  (cp.  $8\text{ m sec}^{-1}$  here) with some occasions reaching  $25\text{ m sec}^{-1}$ .

### 7.2.2 The mean flow and dust

Dust pick-up was widely debated at the workshop. A desiccated surface favours pick-up and a critical pick-up speed which varies from point to point, is required. Dryness is represented in Figure 7.14 by the shaded regions which correspond to rainfall values of less than one centimetre per month. Over the Sahara highest wind speeds from Figure 7.14 occur at  $10\text{--}15^\circ\text{N}$  in winter,  $20^\circ\text{N}$  in spring and  $25^\circ\text{N}$  in late summer. Concomitantly the dry region moves north with season. On these two counts then maximum pick-up is expected to vary seasonally. To show the geographical variation the distribution of mean wind kinetic energy at 850 mb is shown in Figure 7.15. Ideally a better parameter to represent pick-up might be the square of the instantaneous wind speed but this was not available. There is a maximum on each side of the Sahara in January with the largest values south of the Sahara and in West Africa. In July the maximum is in the Northwest Sahara with high values also in the Northeast. The frequency of haze over the ocean is a measure of air-borne



MEAN  $\bar{U}$  AT 850mb - JULY



MEAN  $\bar{U}$  AT 850mb - OCTOBER

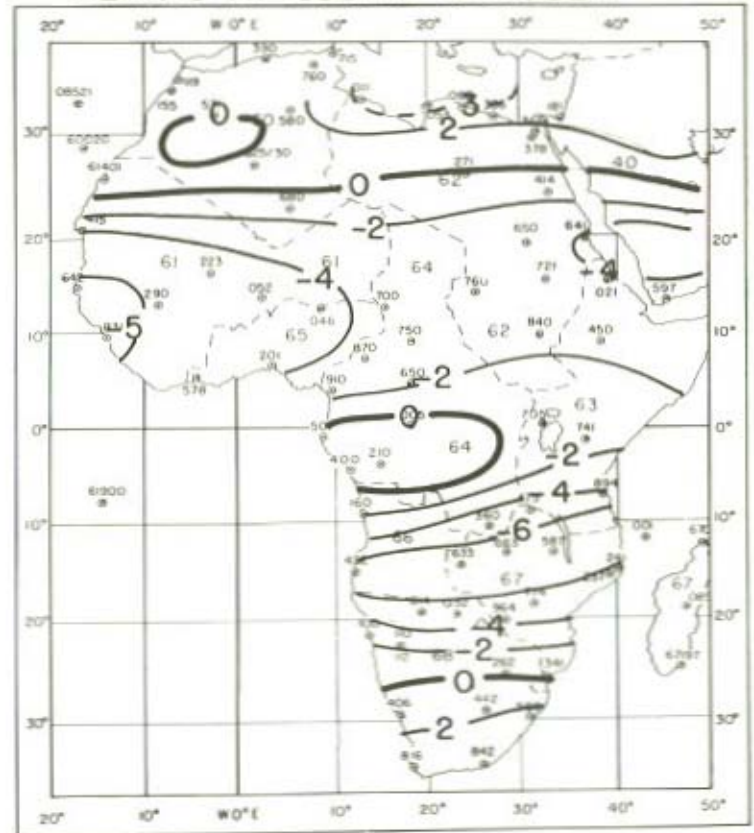
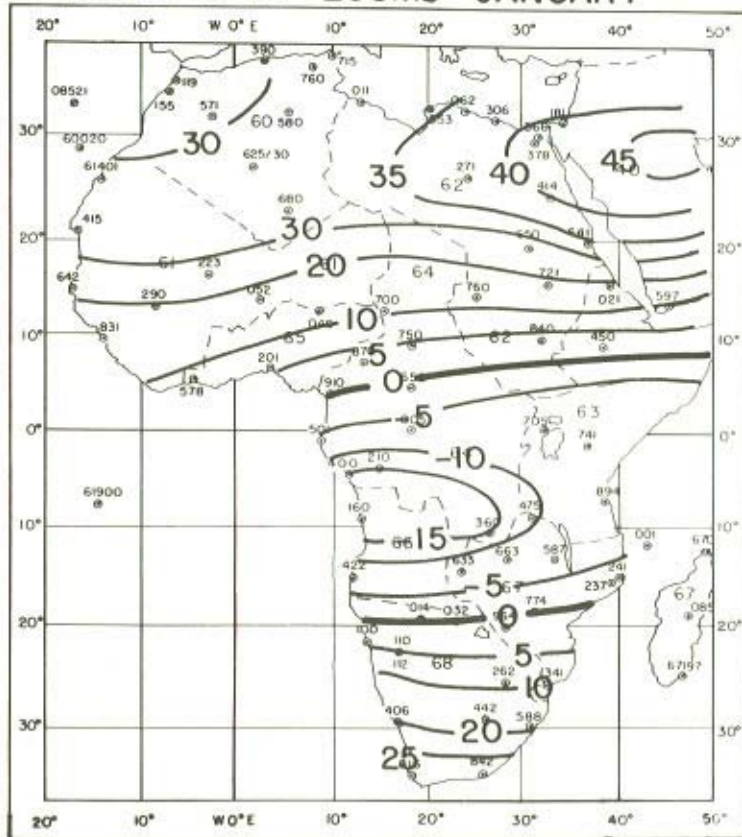
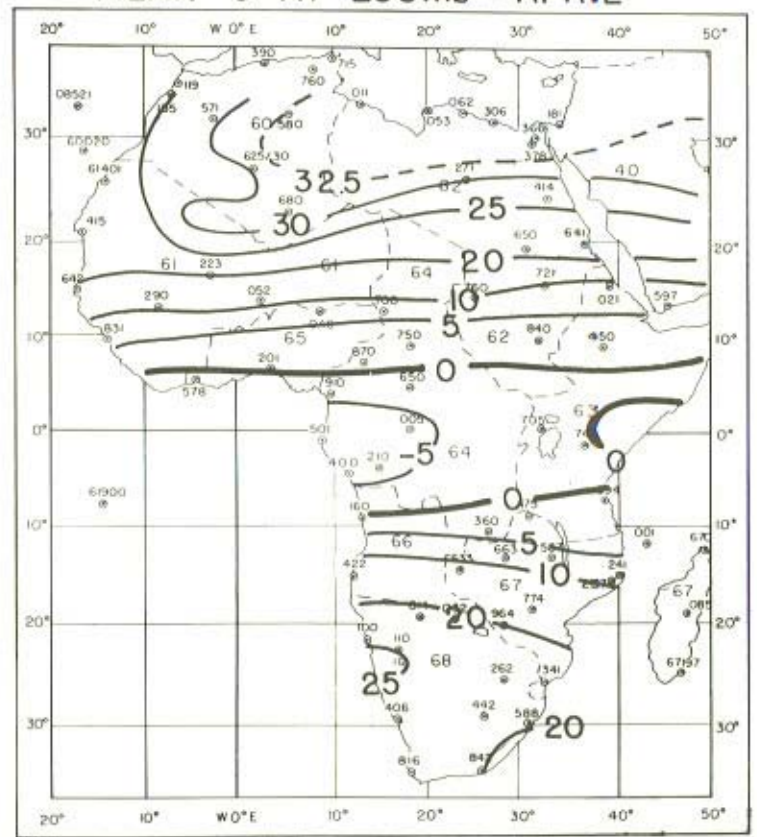


Figure 7.4 Monthly mean wind component  $\bar{U}$  at 850 mb for January, April, July, and October

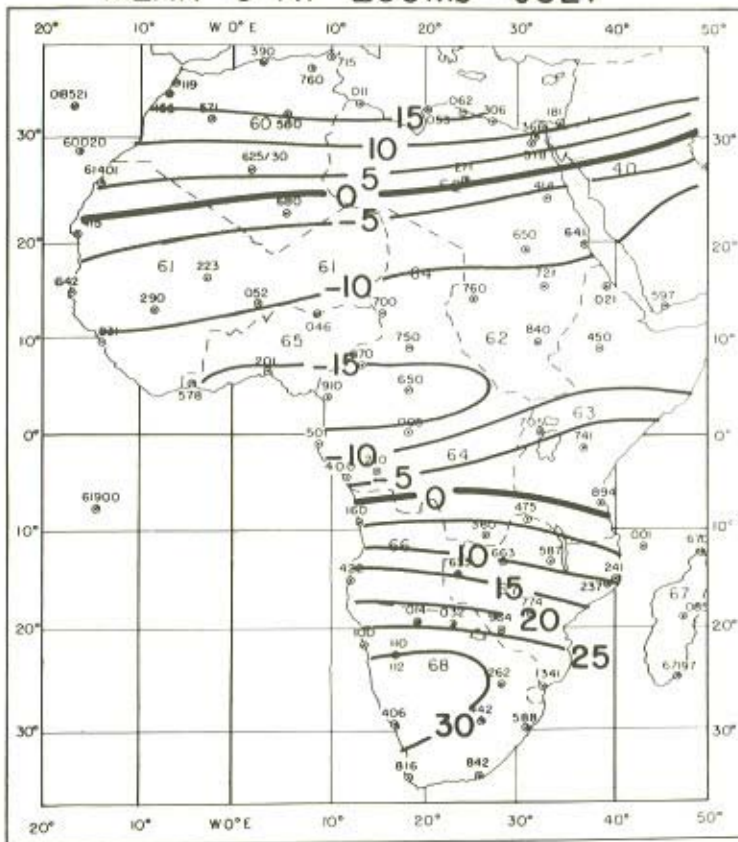
MEAN  $\bar{u}$  AT 200mb - JANUARY



MEAN  $\bar{u}$  AT 200mb - APRIL



MEAN  $\bar{U}$  AT 200mb - JULY



MEAN  $\bar{U}$  AT 200mb - OCTOBER

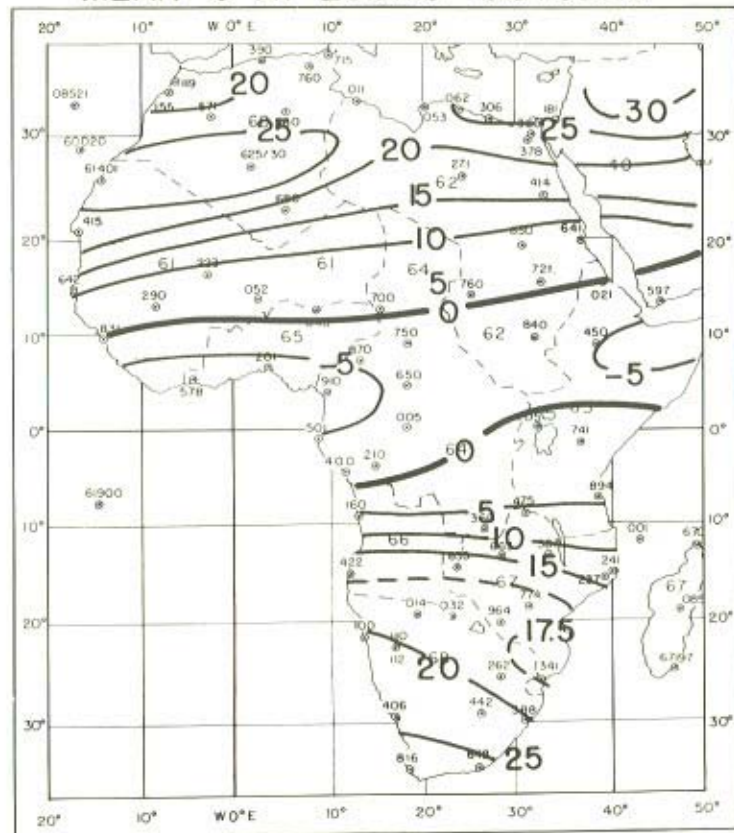
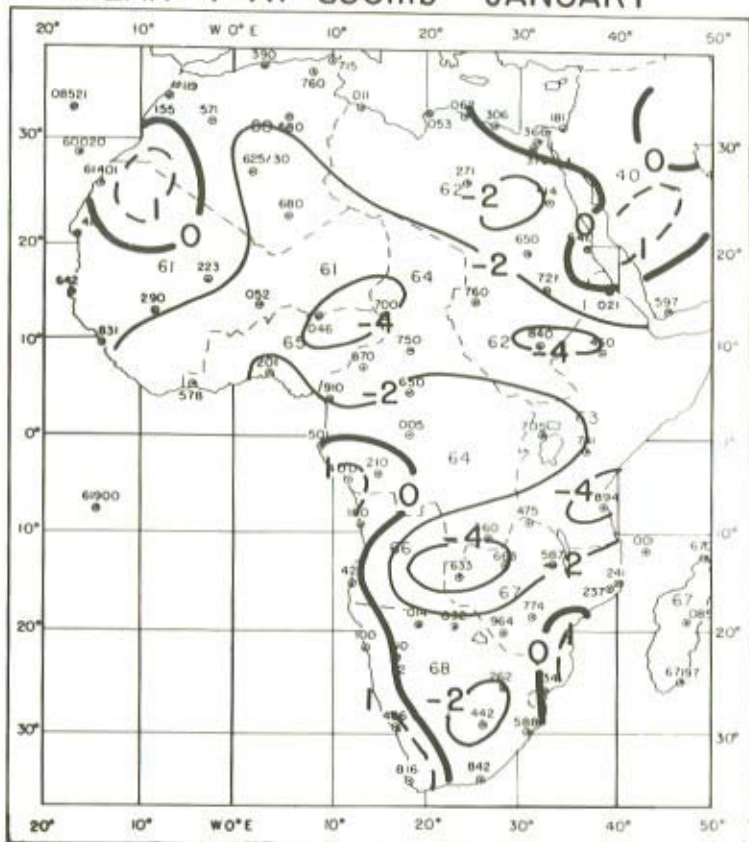
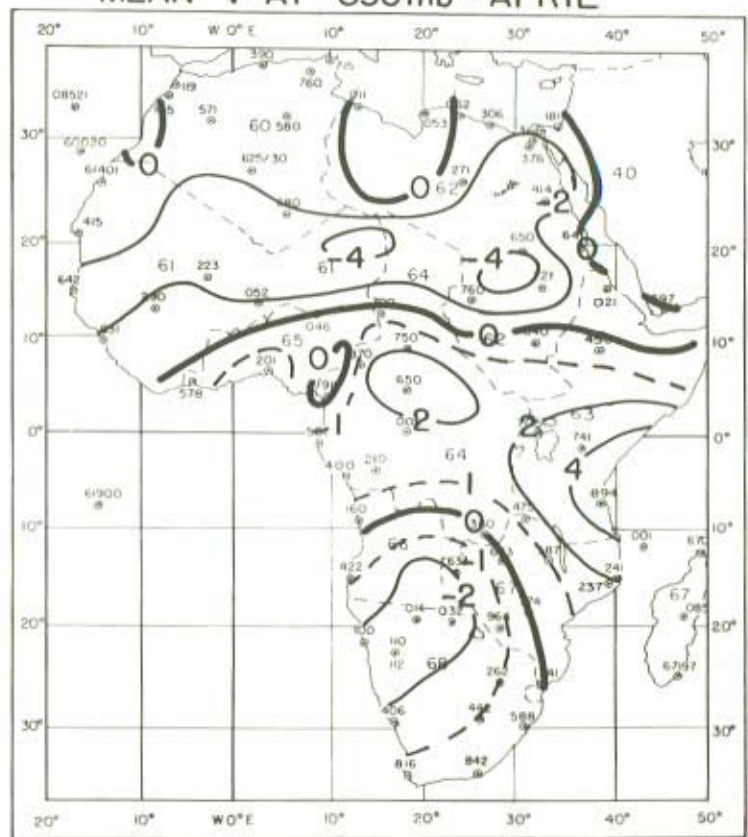


Figure 7.5 Monthly mean wind component  $\bar{U}$  at 200 mb for January, April, July, and October

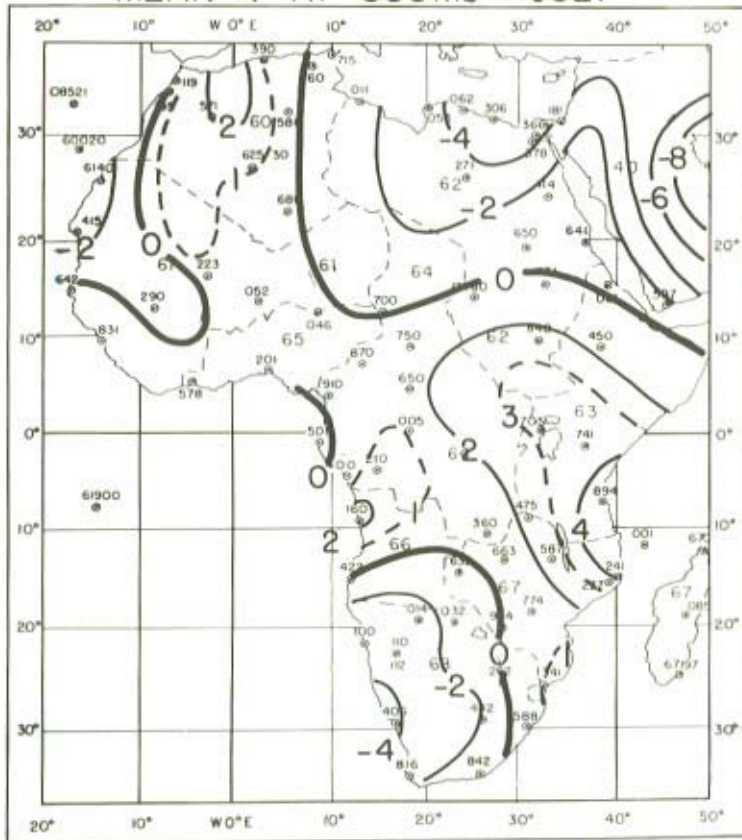
MEAN  $\bar{V}$  AT 850mb - JANUARY



MEAN  $\bar{V}$  AT 850mb - APRIL



MEAN  $\bar{V}$  AT 850mb - JULY



MEAN  $\bar{V}$  AT 850mb - OCTOBER

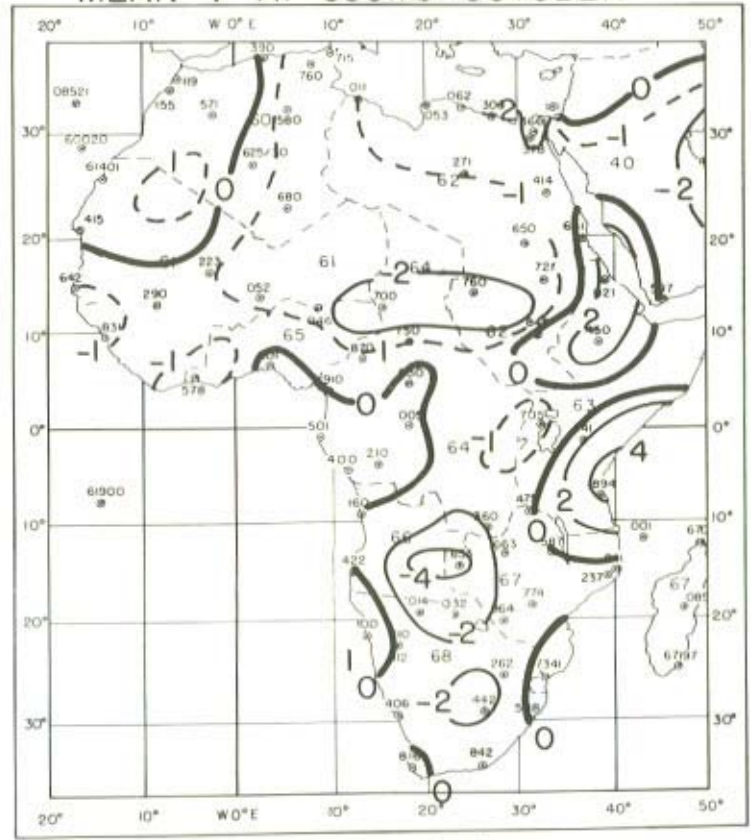
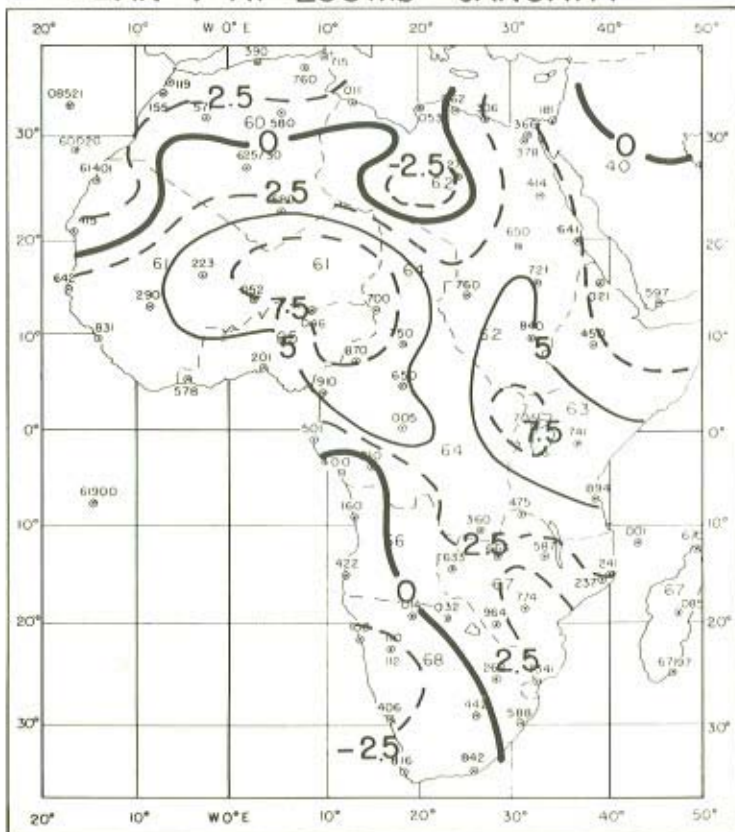
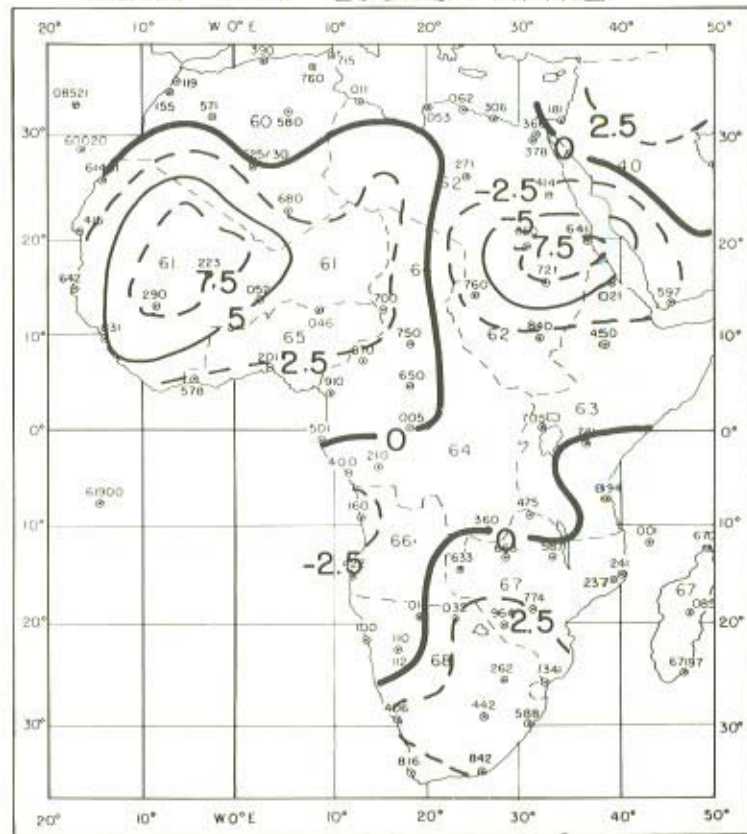


Figure 7.6 Monthly mean wind component  $\bar{V}$  at 850 mb for January, April, July, and October

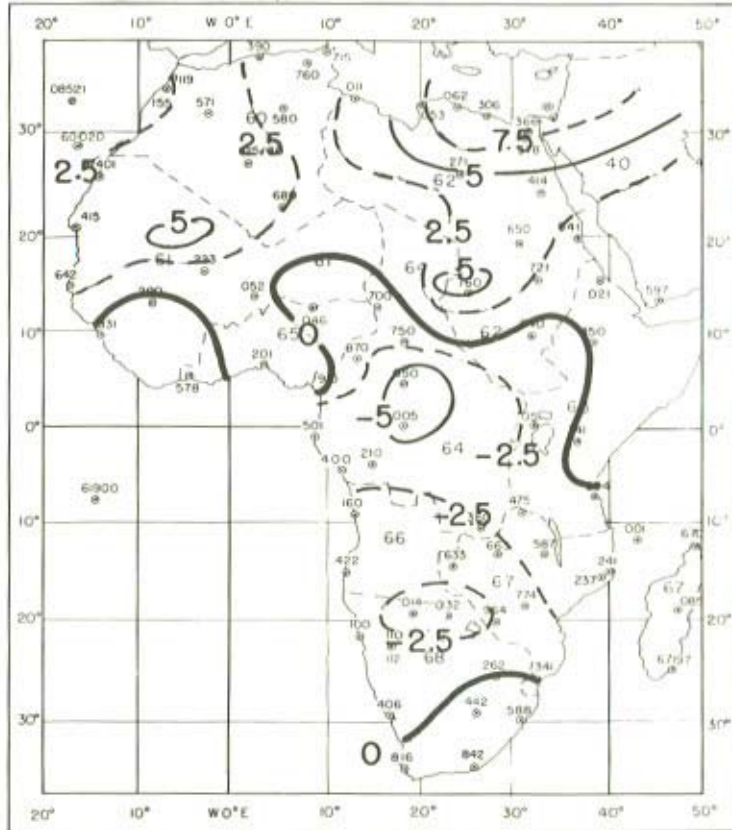
MEAN  $\bar{V}$  AT 200mb - JANUARY



MEAN  $\bar{V}$  AT 200mb - APRIL



MEAN  $\bar{V}$  AT 200mb - JULY



MEAN  $\bar{V}$  AT 200mb - OCTOBER

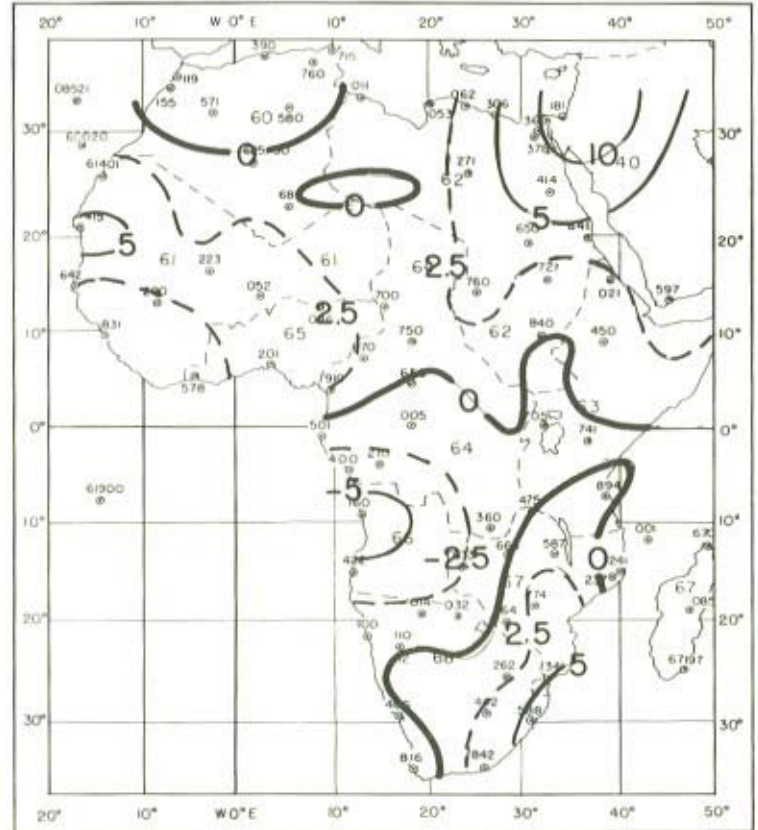


Figure 7.7 Monthly mean wind component  $\bar{V}$  at 200 mb for January, April, July, and October

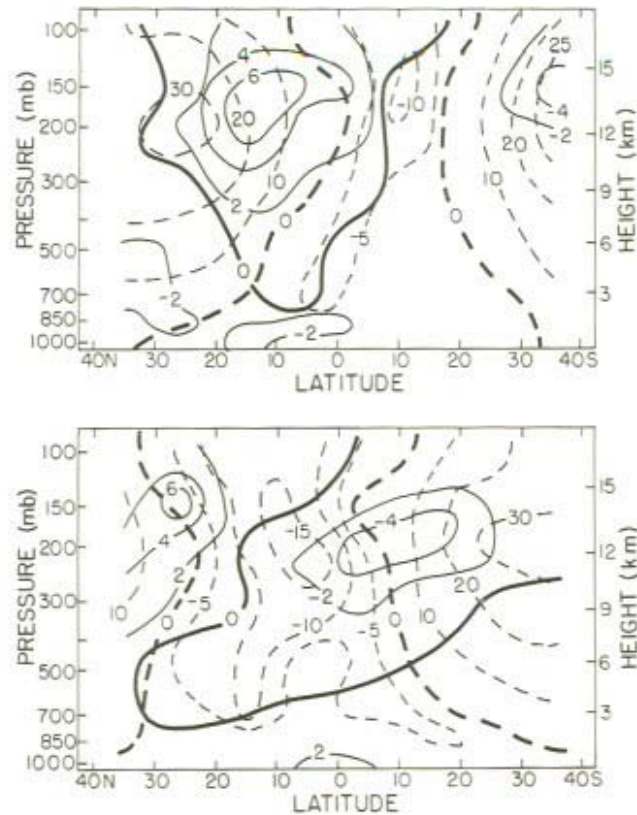


Figure 7.8 Zonal and meridional wind components for  $0^{\circ}$  longitude (Units:  $\text{m sec}^{-1}$ ) Top: January. Bottom: August  
Key: - - - Zonal — Meridional

dust, and data compiled in the 1930's are shown in Figure 7.16. In northern winter considerable dust blows westward from the southern Sahara. Kalu (1979) presented evidence that the alluvial plain of Bilma (Niger)/Faya Largeau (Chad) is a major source in winter. In summer the peak haze frequency lies further north and in addition there is a massive transport towards the east, as might be anticipated from the occurrence of dry westerlies at  $40^{\circ}\text{E}$  longitude in that season (Figure 7.11). In southern Africa there is a correspondence between dry easterlies at  $20\text{--}25^{\circ}\text{S}$  throughout the year, and the occurrence of marine haze. The use of 850 mb seems appropriate as much of the dust is confined to the lowest 3 km (Prospero and Carlson, 1972). In general terms then the mean wind kinetic energy pattern, the mean flow pattern and the rainfall can be said to give a first order explanation of the marine visibility maps, but more cannot be said without knowledge of the detailed distribution of the sources and, as Kalu stressed, detailed distribution of

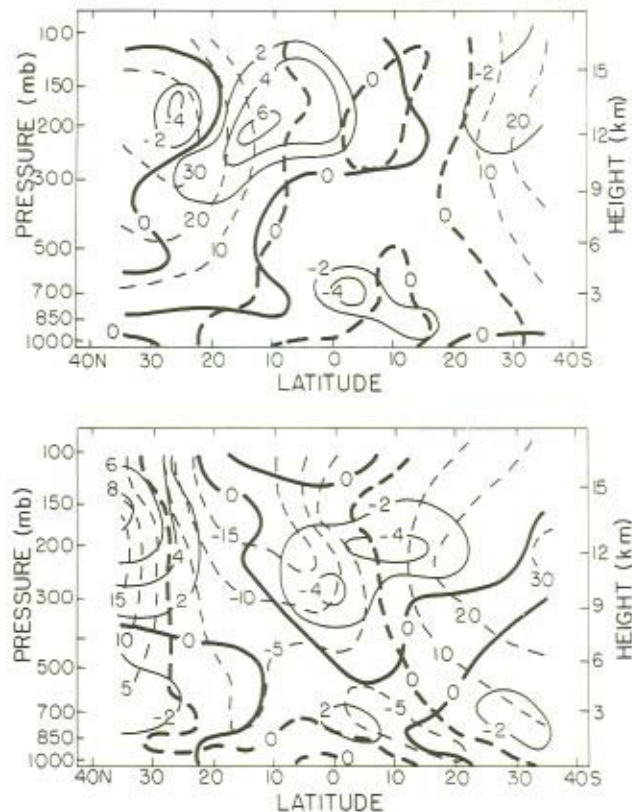


Figure 7.9 Zonal and meridional wind components for 20°E longitude (Units:  $\text{m sec}^{-1}$ ) Top: January. Bottom: August  
Key: - - - - Zonal ——— Meridional

the surface wind. Insofar as the mean flow pattern represents the sum of the passage of transient eddies then it can be used to represent the dust transport, but for pick-up it was stressed at the meeting that power law values of the instantaneous surface wind speed may be involved (e.g. Gillette, 1979), which would not be adequately represented by mean values.

### 7.2.3 Moisture

There is a substantial variation with season in moisture over the desert as shown in Figure 7.17. Lowest values occur in association with the largest sinking motion (cf. Figure 1) as might be expected.

In the early studies of water vapour transport problems by the Planetary Circulations Project directed by the late Professor Victor P. Starr, transport over

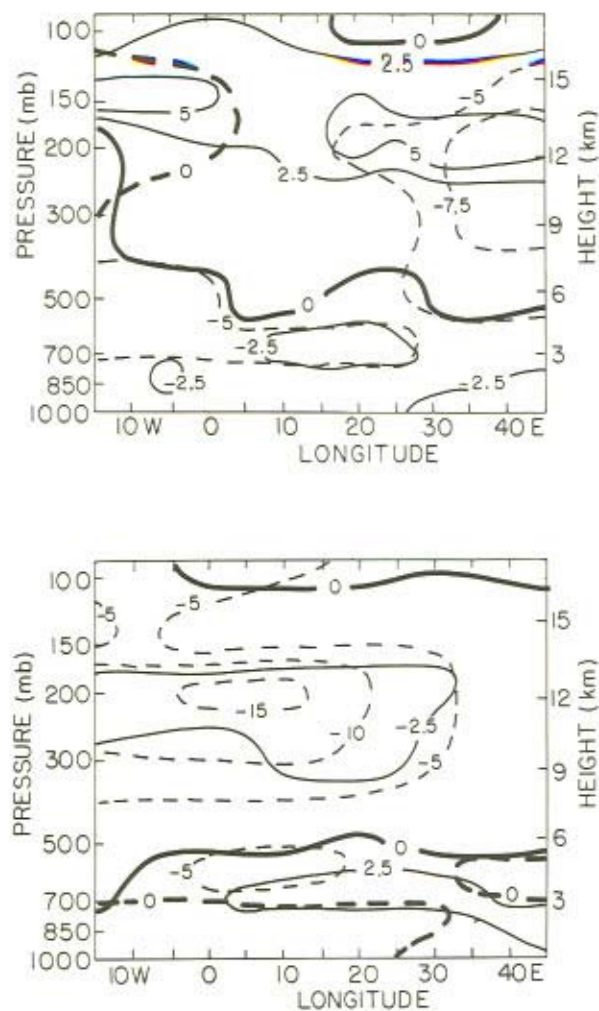


Figure 7.10 Zonal and meridional wind components for equatorial plane (Units:  $\text{m sec}^{-1}$ ) Top: January. Bottom: July.  
Key: - - - Zonal — Meridional

Africa was treated as a part of the hemispheric or global problem (e.g. see Peixoto, 1973). A few works have focused on Africa, for example, those by Flohn *et al.* (1965) and Peixoto and Obasi (1965). A general finding was that, as for other tropical regions, mean motions contributed most to the total flux, as opposed to day-to-day eddy motions, so that monthly mean winds could be used in association

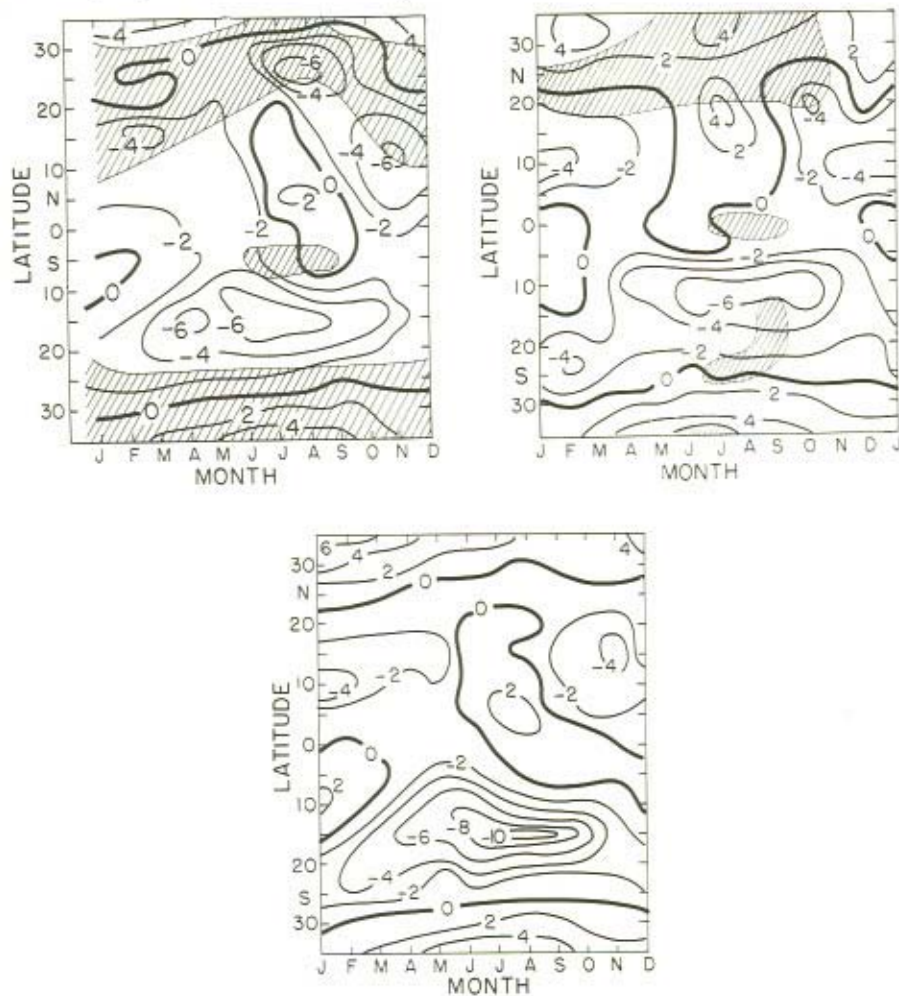


Figure 7.11 Time latitude sections of mean zonal wind at the 850 mb level at  $0^\circ$ ,  $20^\circ\text{E}$ , and  $40^\circ\text{E}$  longitude (Units:  $\text{m sec}^{-1}$ . Shaded areas: Rainfall  $< 1$   $\text{cm/month}$ ) Left:  $0^\circ$ . Centre:  $20^\circ\text{E}$ . Right:  $40^\circ\text{E}$

with monthly mean moisture contents to compute the mean flux. The transport components are:

$$Q_\phi = \frac{1}{g} \int \bar{q} \bar{v} dp$$

$$Q_\lambda = \frac{1}{g} \int \bar{q} \bar{u} dp$$

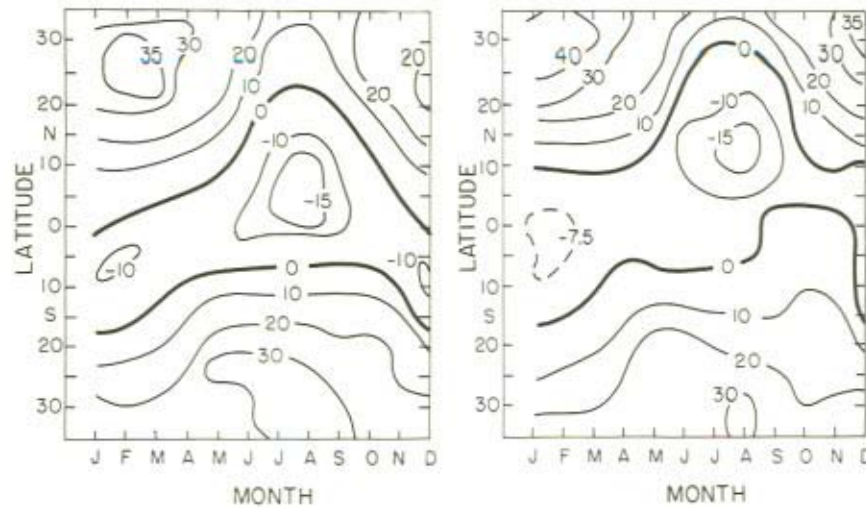


Figure 7.12 Time latitude sections of mean zonal wind at the 200 mb level at  $0^\circ$  and  $40^\circ\text{E}$  longitude. (Units:  $\text{m sec}^{-1}$ ) Left:  $0^\circ$ . Right:  $40^\circ\text{E}$

where  $\phi$  and  $\lambda$  are latitude and longitude and  $\bar{q}$  is the monthly mean specific humidity (in  $\text{gm/kg}$ ). The streamlines of the vertically integrated flux computed by Kidson (1977) are shown in Figure 7.18. These streamlines represent the non-divergent part of the flow; the divergent part,  $\nabla \cdot \mathbf{Q}$ , is also shown. In the early part of the year the moisture over the Northern Sahara originates from the Atlantic while in summer the origin is the Mediterranean area. Moisture over the Sahel also travels from the Mediterranean in the beginning of the rainy season, but later the Indian ocean region becomes a source. The pattern is quite different from that which would be inferred from the surface streamlines.

In general dust, like water vapour, will be concentrated in the lower troposphere and it seems reasonable to assume that the transport is also mainly by the mean winds. The climatological data presented here could therefore be used in the assessment of station sites.

Mean rainfall patterns are shown in a number of climatological texts (e.g. Thompson, 1965; see also Kidson, 1977). These give a guide to regions which are vulnerable to surface pick-up and they also represent a measure of a major sink, washout. In the lower rainfall periods of 1972–73 more dust could be picked up because of dry surfaces and less dust would be removed by rainfall, than in the wetter years in the early 1960's.

Examples of the time variations of rainfall are shown in Figure 7.19 in a form that may be used in wash-out computations.

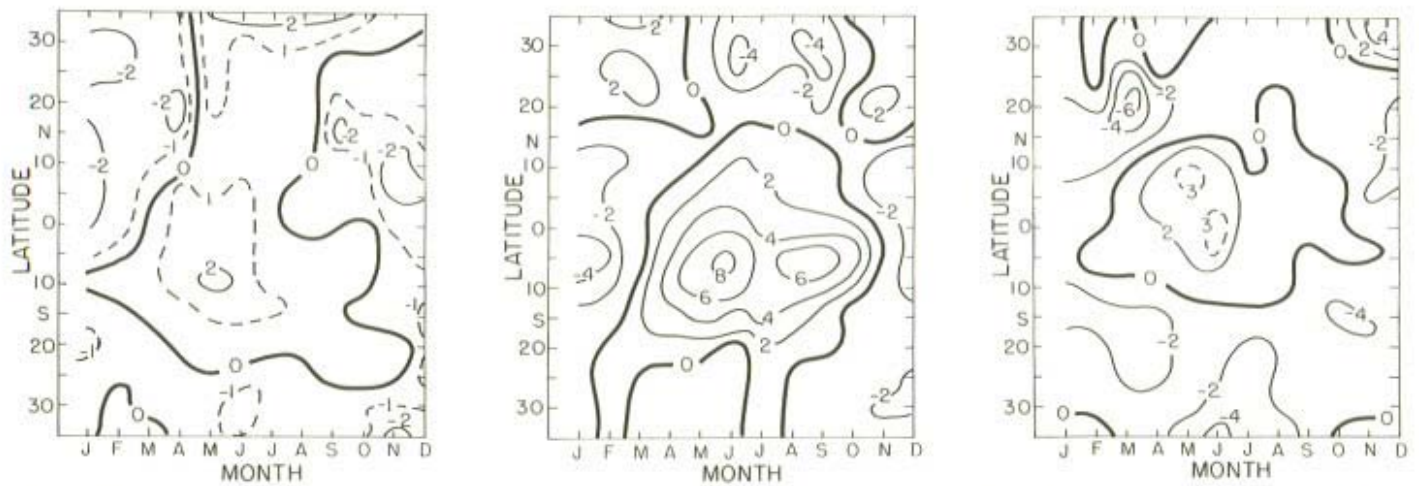


Figure 7.13 Time latitude sections of mean meridional wind at the 850 mb level at 0°, 20°E, and 40°E longitude (Units: m sec<sup>-1</sup>) Left: 0°. Centre : 20°E. Right: 40°E

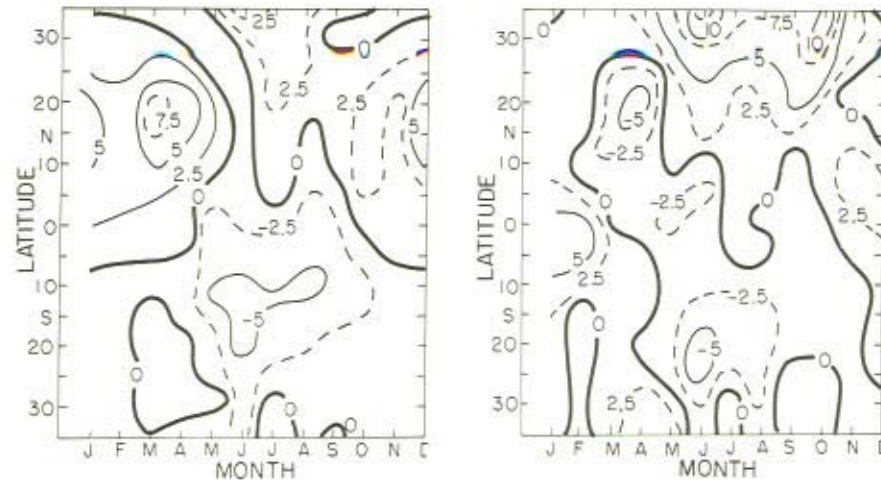


Figure 7.14 Time latitude sections of mean meridional wind at the 200 mb level at  $0^{\circ}$  and  $40^{\circ}$ E (Units:  $\text{m sec}^{-1}$ ) Left:  $0^{\circ}$ , Right:  $40^{\circ}$ E

### 7.3 YEAR-TO-YEAR CHANGES

#### 7.3.1 Wind velocity

The details of the monthly mean tropospheric flow patterns vary from year to year. The interest here is between predominantly wet and dry years, the latter with more potential for dust pick-up. Elsewhere Kidson (1977) has presented streamlines for 850 and 200 mb for August 1959 and 1961 (wet years) and August 1972 and 1973 (dry years) (Figure 7.20) and has pointed out that the 850 mb trough normally present at about  $8^{\circ}$ N in the wet years was absent in the dry years. The easterlies at 200 mb are also a good deal weaker in the dry years as may be seen also from the individual year equatorial cross-sections of Figure 7.21. The meridional flow which produces these easterlies is also a little weaker in 1973.

#### 7.3.2 Moisture

Rainfall variations between wet and dry years of the recent period have been discussed by several authors (e.g. Winstanley, 1973; Sircoulan, 1974; Tanaka *et al.*, 1965; Bunting *et al.*, 1976; Kidson, 1977). The main rain region over West Africa moves north and south in a regular fashion reaching its northernmost position in August. The centre of gravity of this part of the rainbelt ( $15^{\circ}$ W to  $25^{\circ}$ E) is shown in Figure 7.22. The dashed line shows the long term mean northernmost position in August. The belt was even further north in 1952, 1956, 1958 (for two months) and 1959 and was south of average in 1966 and 1968. But clearly there has not been a

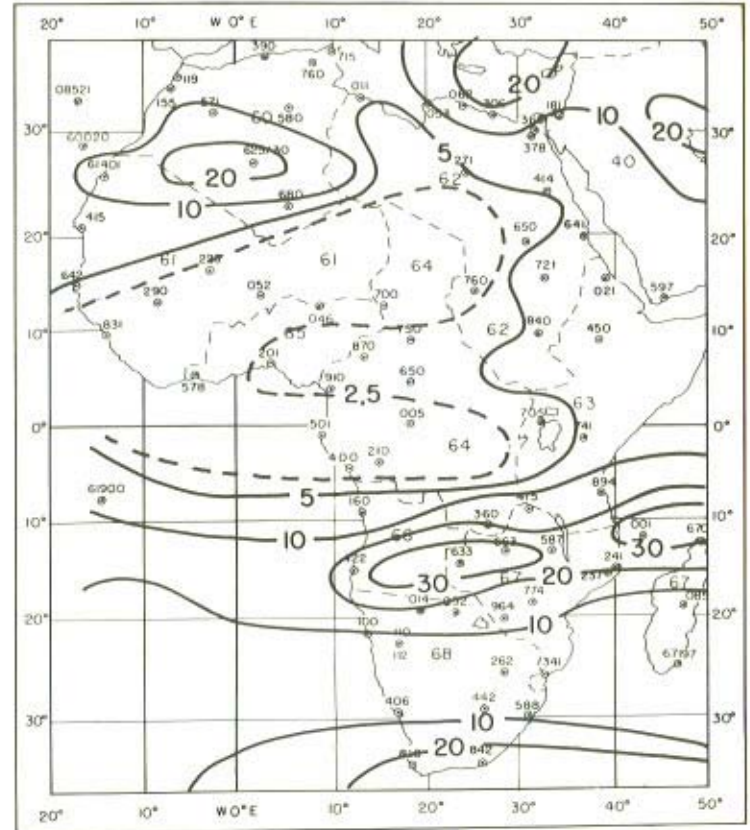
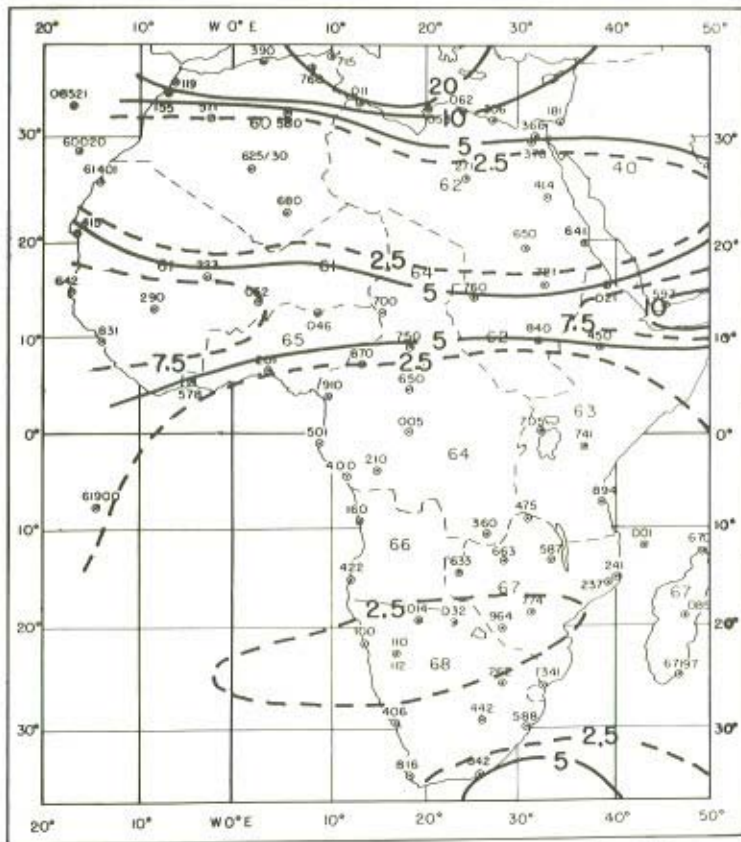


Figure 7.15 Kinetic energy of the mean wind  $(\bar{U}^2 + \bar{V}^2)/2$  at 850 mb January and July (Units:  $\text{m}^2 \text{sec}^{-2}$ ) Left: January. Right: July

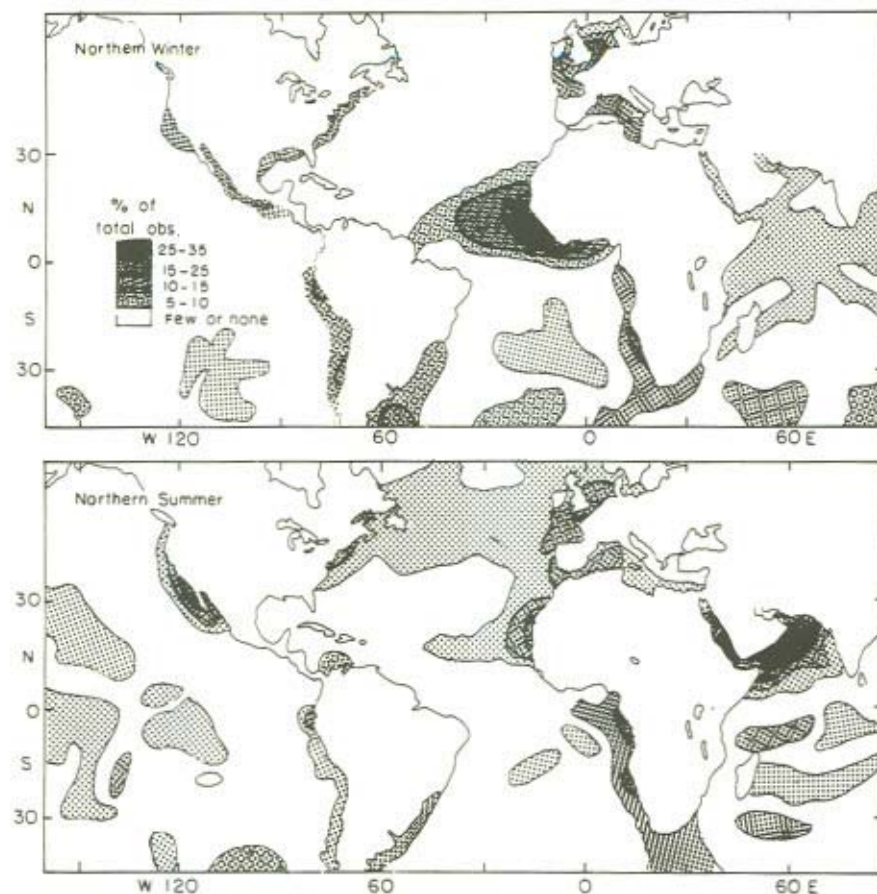


Figure 7.16 Frequency of haze over the oceans (after Turekian, 1968)

systematic drift southwards and it may be rather that it is the overall intensity of the Hadley cell circulation that is weaker in years of low rainfall.

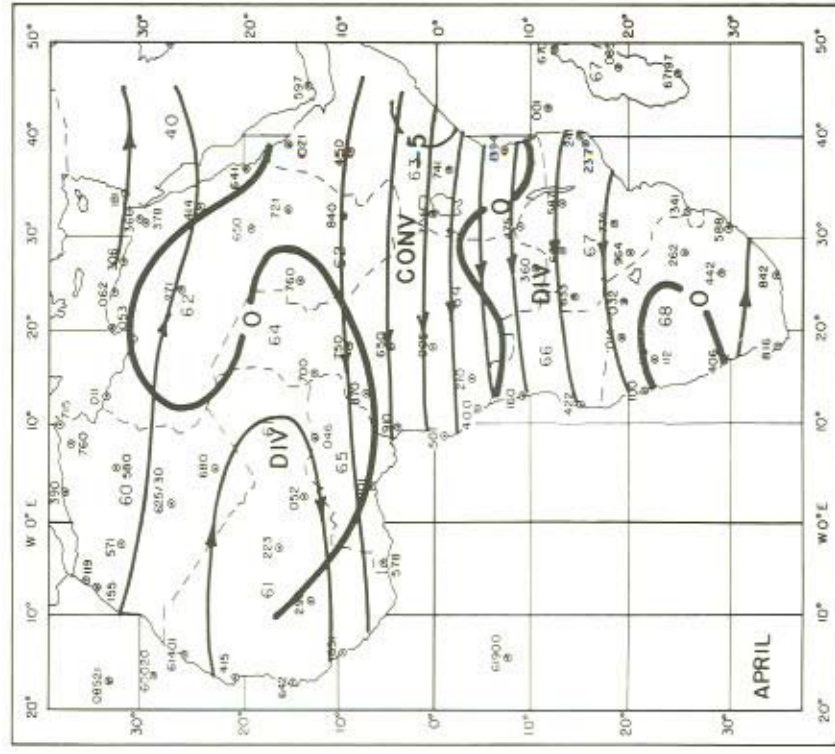
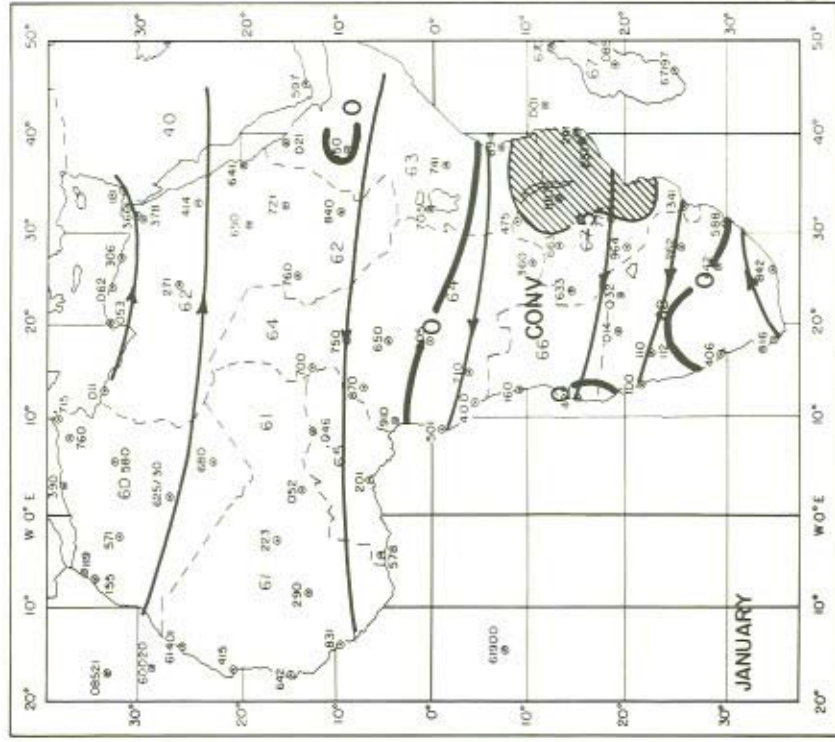
The specific humidity pattern shows evidence of slightly lower values in 1973 than 1959 (Figure 7.23) in maximum regions, near the strongest rising motion, and at 25°N near the northern hemisphere sinking motion.

Relationships with sea surface temperature in the adjoining Atlantic and the Indian Ocean were also sought but there were no strong correlations, although our data sample spanned only the period 1949–69, so we did not have a good sample of sea temperature for the dry years.

### 7.3.3 Dust

According to the presentation of Prospero (1979) there have been changes in the summer dust content of air over the Atlantic. The summer dust appears to originate







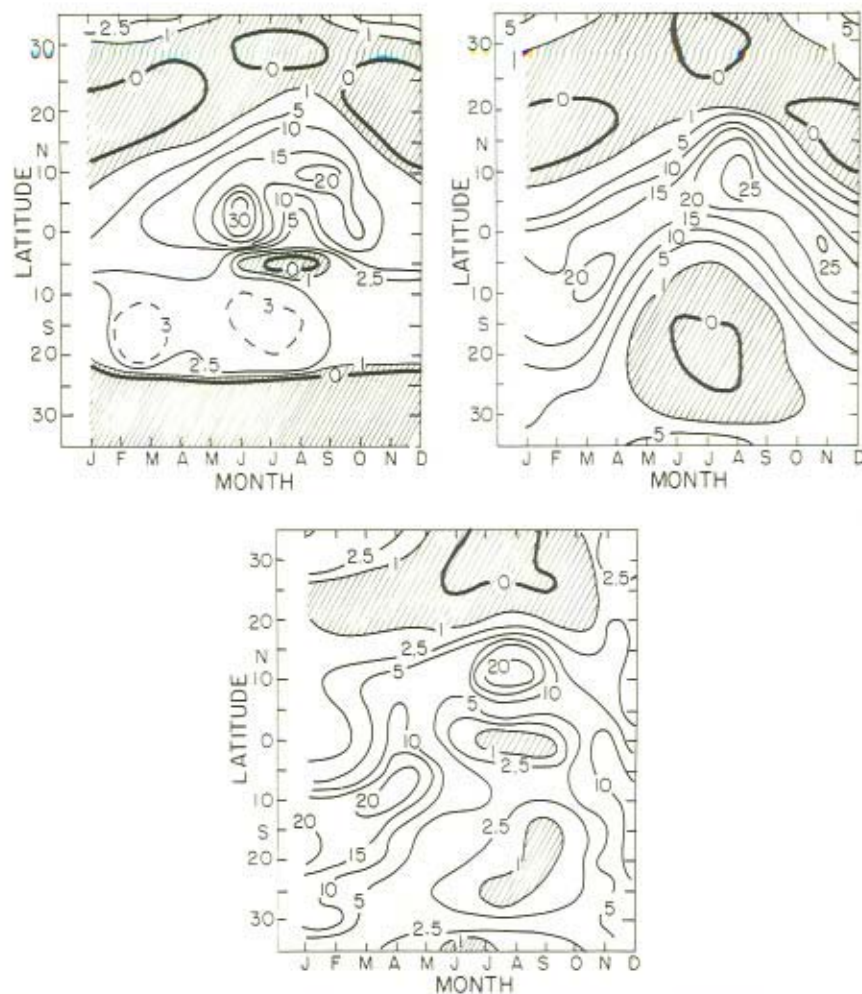


Figure 7.19 Monthly rainfall vs. latitude at  $0^{\circ}$ ,  $20^{\circ}\text{E}$ , and  $40^{\circ}\text{E}$  (Units: cm/month) Left:  $0^{\circ}$ . Centre:  $20^{\circ}\text{E}$ . Right:  $40^{\circ}\text{E}$ . Shaded areas show rainfall  $< 1$  cm/month

from the central and northern Sahara according to Section 7.2.2 above and may therefore be expected to be of the red type (Rapp, 1974). While changes in the summer are not so likely to be related to the Sahel they may be governed by circulation changes which we find over all of Africa north of the equator.

#### 7.3.4 Relationship between drought and global temperature

It was pointed out elsewhere that surface temperature near  $15^{\circ}\text{N}$  increased during the drought years and it was suggested that this was due to planetary albedo

changes (Tanaka *et al.*, 1975). Possible relationships with free air temperature have also been examined. Monthly mean temperature data from 150 upper air stations for the period 1958–74 have been subjected to an empirical orthogonal function analysis to bring out the patterns of the non-seasonal changes. Only stations with at least 80% of the data present were included in the analysis which was performed for levels of 850 mb, 500 mb, and 200 mb. This analysis is to be described elsewhere (Weare, Kidson, Navato, and Newell, *Unpublished Ms.*, 1977). The first ten functions at each level were incorporated in a screening regression procedure to examine their relationship to changes in July to September rainfall in Africa. The patterns most strongly related to the rainfall changes are obtained by combining the EOF patterns with weights given by the screening regression procedure and are shown in Figures 7.24 and 7.25 (after Kidson, 1977).

The 850 mb temperature pattern implies that free air temperature is lower over Africa in the wet years as was found for the surface. In the dry years soil desiccation would be favoured at the higher temperatures. The 200 mb pattern shows evidence of stronger meridional temperature gradients in both hemispheres in wet years. This is consistent with the suggestion of Section 7.3.2 that it is the overall *intensity* of the Hadley cell circulation that is weaker in years of low rainfall.

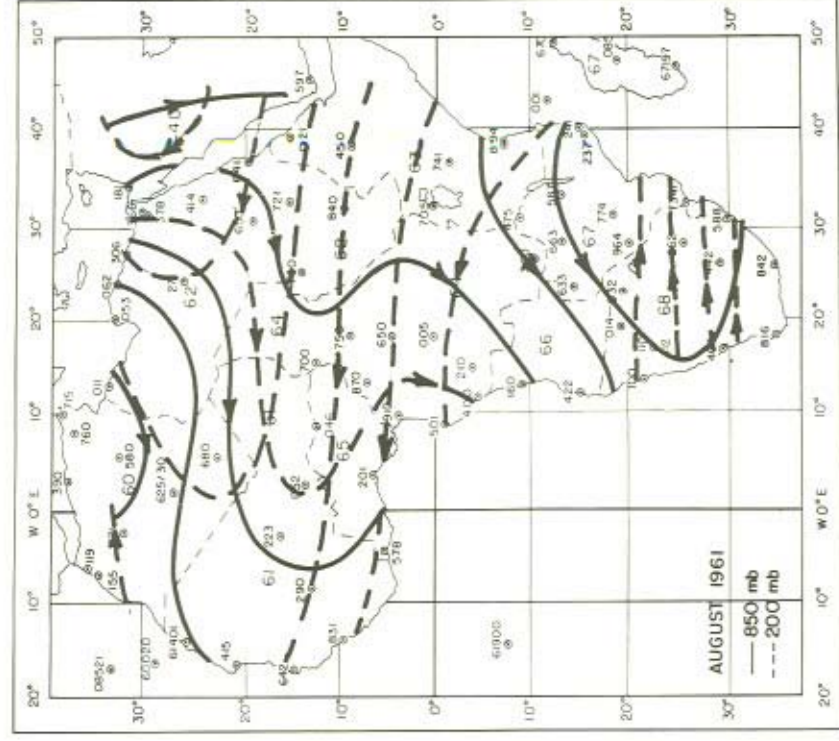
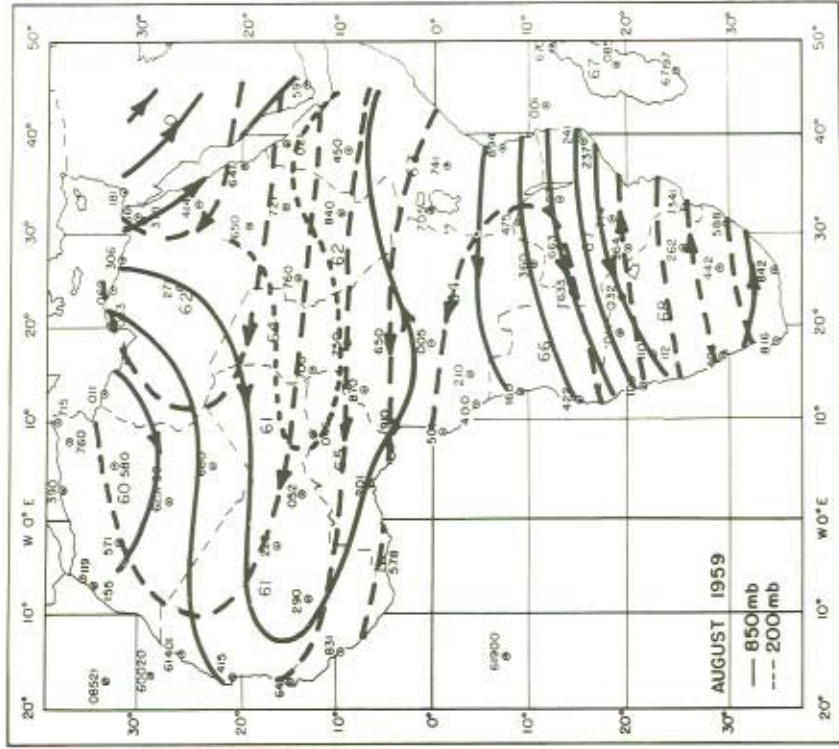
The source of the enhanced tropospheric temperature gradients is still a mystery. Modulation of sea surface temperature is a possibility, but, as noted, data subsequent to 1969 for the Atlantic and Indian oceans is not yet available.

#### 7.4 CONCLUDING REMARKS

The mean flow patterns over Africa have been presented in horizontal and vertical sections. The broad-scale features of the patterns of dust over the sea can be attributed to the mean flow although the actual pick-up may be more closely related to the transient circulations.

Between the moist regime in the Sahel in the late 1950's and the dry regime of the early 1970's there are significant changes in the flow patterns. There are related changes in the rainfall patterns which seem best described in terms of a reduction in the Hadley cell circulation intensity. Temperature patterns show evidence of high values at the surface and at 850 mb in dry years. The meridional temperature gradients at 200 mb are weaker in both hemispheres in dry years which is consistent with an observed reduction in intensity. We do not know the reason for these gradient changes.

Eolian transport of African dust and its variability in deep sea cores has been used by Parkin and Shackleton (1973) to assess the 'vigour' of the circulation during ice ages. For Atlantic core V23–100 (21°N, 23°W) they deduce stronger trade winds during the cold periods. It has been argued that latitudinal temperature gradients were also greater during cold periods (Newell, 1973). However, from the present findings, it must be borne in mind that trajectory changes could equally well be to blame for the observed dust changes.



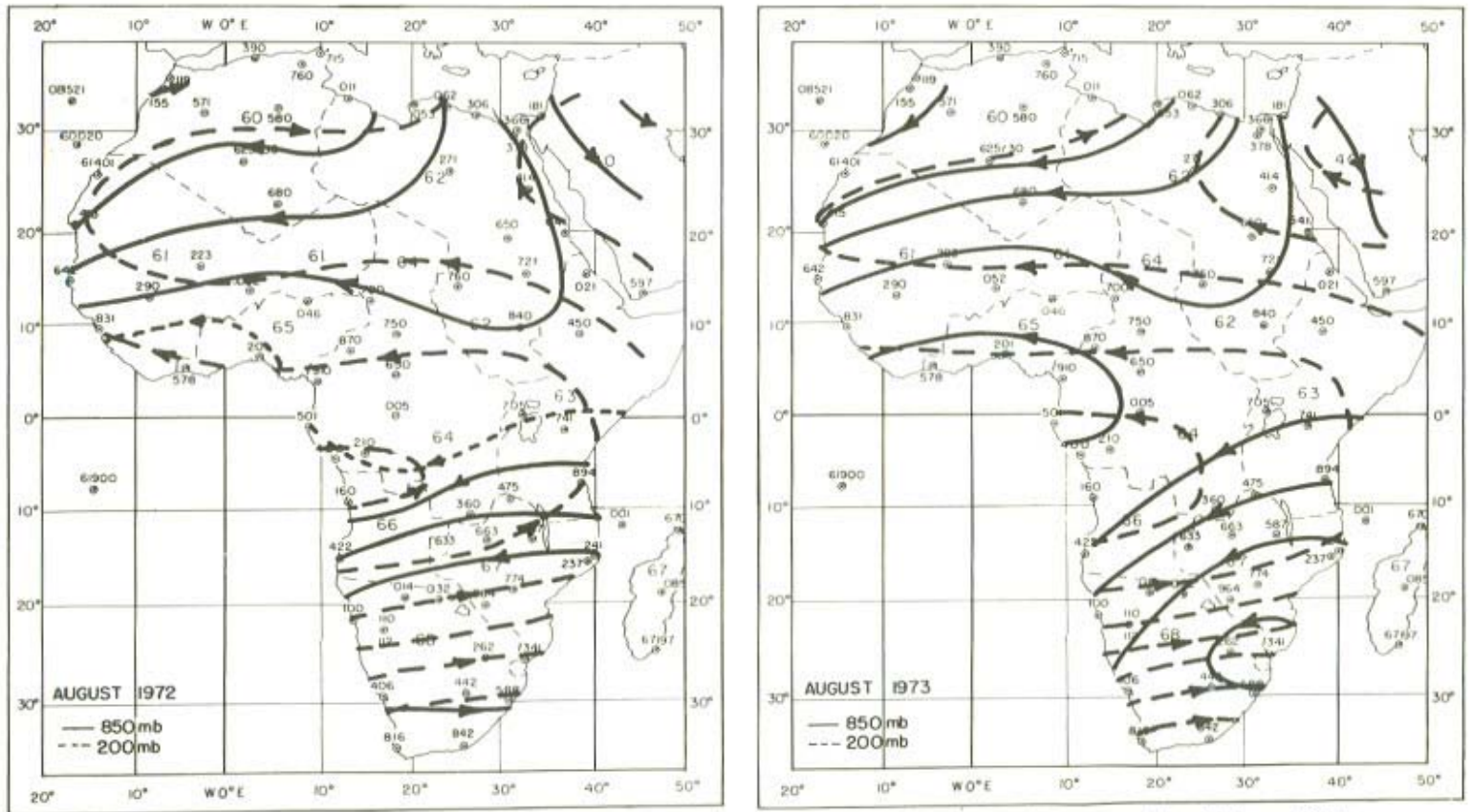


Figure 7.20 Streamlines of the August circulation at 850 mb and 200 mb for wet and dry years (after Kidson, 1977)

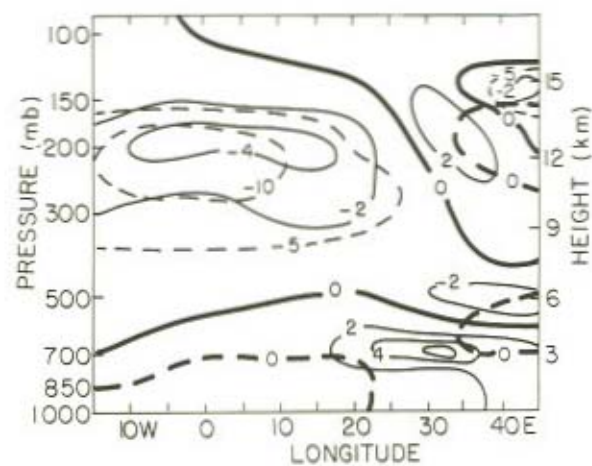
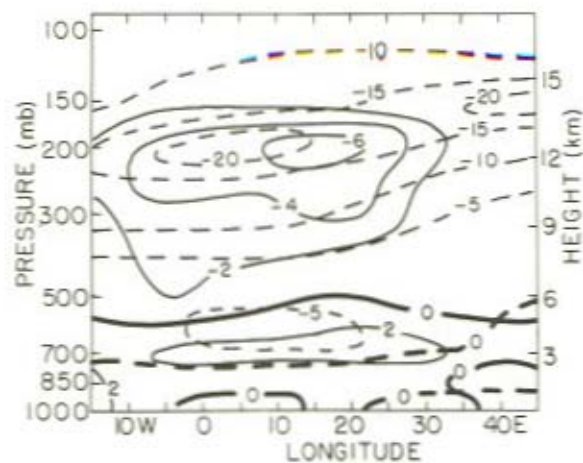


Figure 7.21 Zonal and meridional wind components in the equatorial plane for August 1959 (wet) at top and August 1973 (dry) at bottom (Units:  $\text{m sec}^{-1}$ )  
Key: --- Zonal  
— Meridional

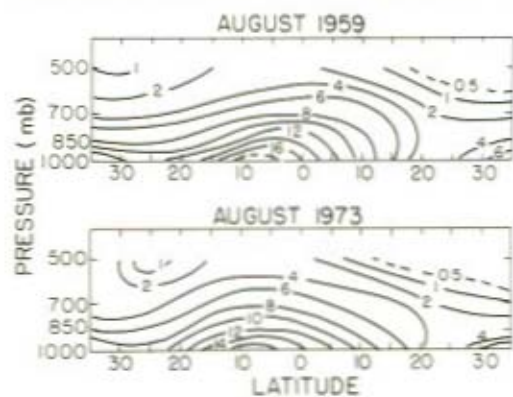


Figure 7.23 Specific humidity for August 1959 (wet) and August 1973 (dry) at  $20^\circ\text{E}$  longitude (Units:  $\text{gm/kg}$ )

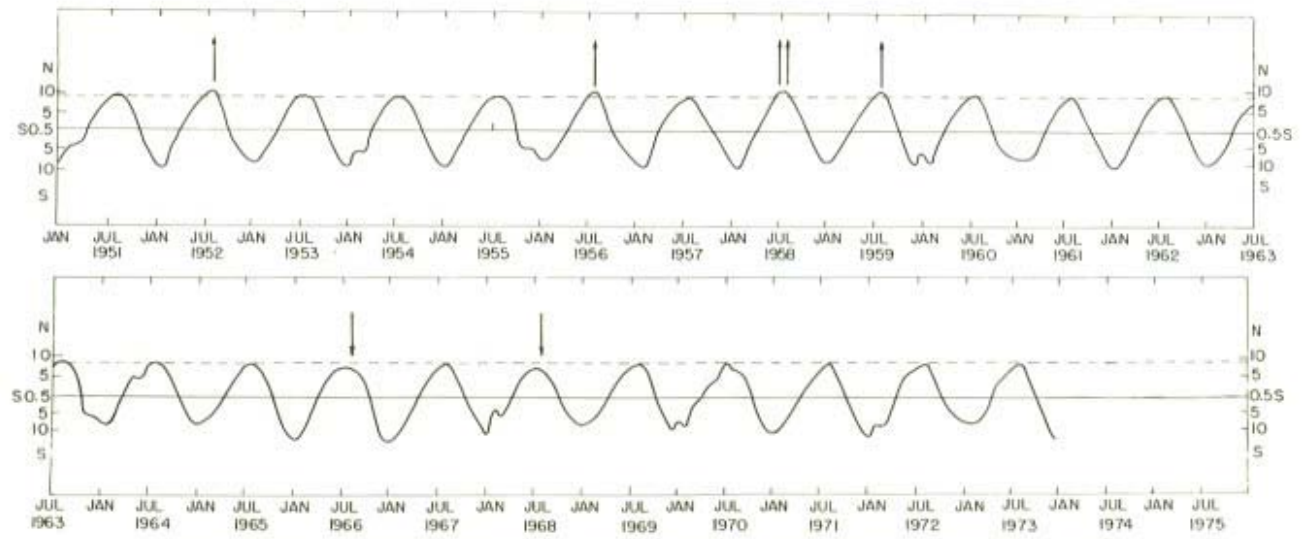


Figure 7.22 Latitude of the centre of gravity of African rainbelt from 1951 to 1973

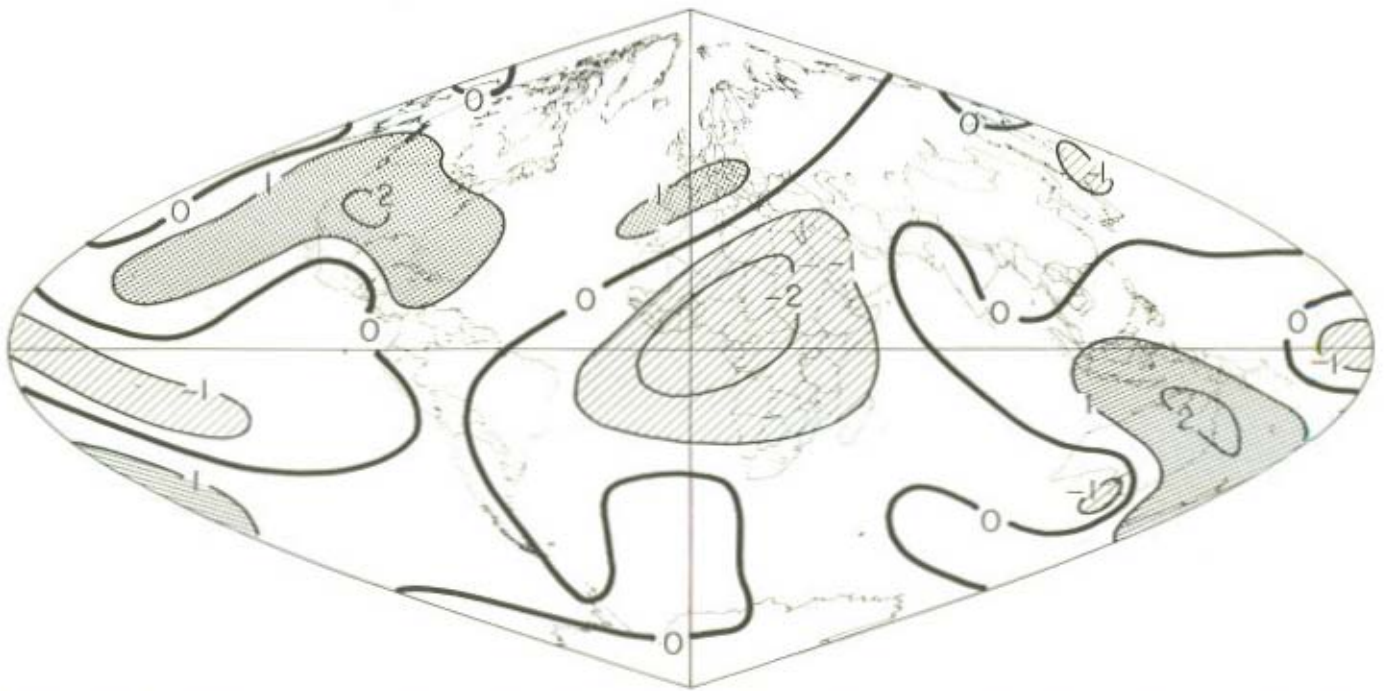


Figure 7.24 Weighted empirical orthogonal function pattern for 850 mb. This pattern results from combinations of the first ten patterns at each level with weights selected by screening regression (after Kidson, 1977)

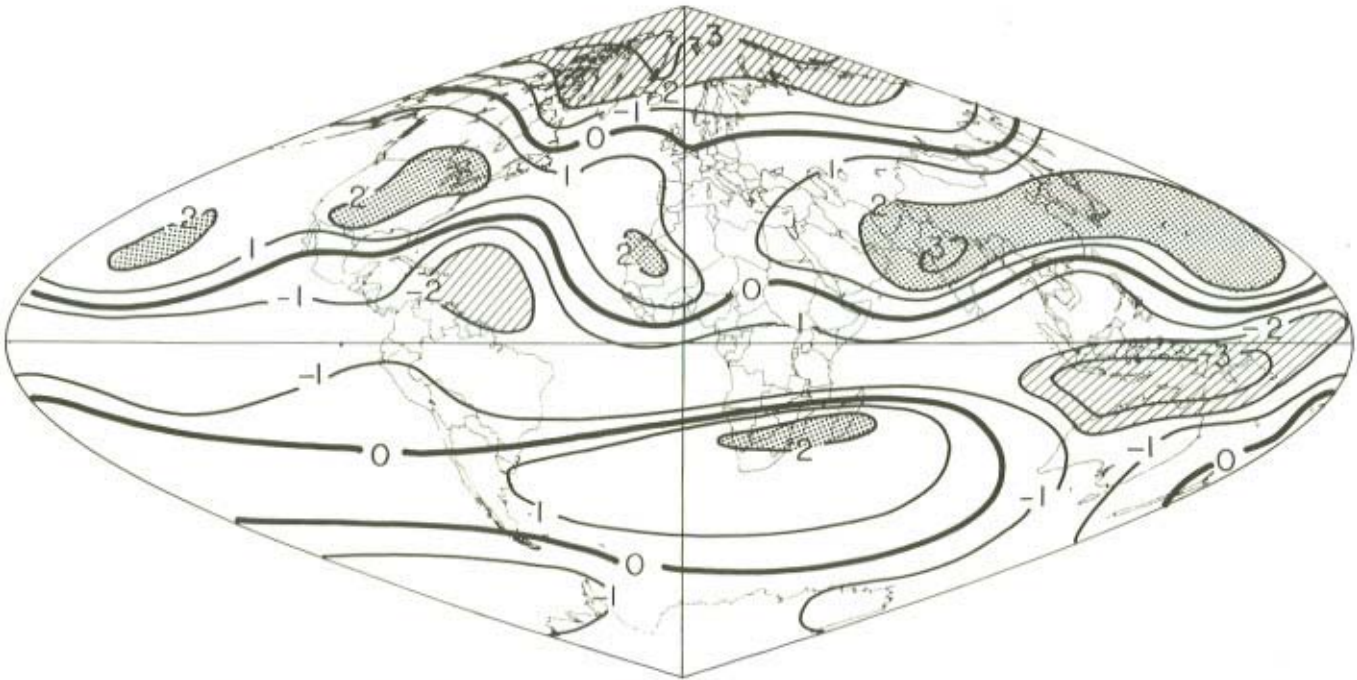


Figure 7.25 Weighted empirical orthogonal function pattern for 200 mb. This pattern results from combinations of the first ten patterns at each level with weights selected by screening regression (after Kidson, 1977)

According to the work of Street and Grove (1975) who have made a careful study of lake-level fluctuations, all of Africa between the equator and 30°N was very wet in the 1000-year period starting at about 9000 B.P. and the dust in ocean cores for that period could be examined as a separate verification. They postulate that sea surface temperature was high at that time. Maley (1976) has also made some pollen analyses which give evidence of the translation of the Hadley cell circulation and even if the intensity change argument is used for the recent period it cannot be extrapolated backwards in time – it is quite possible that the translation argument holds on the 10,000-year time scale.

### 7.5 ACKNOWLEDGMENTS

We thank Dr. B. C. Weare and Dr. A. Navato for their participation in the free air temperature study.

We gratefully acknowledge research support from the United States Energy Research and Development Administration under Contract E(11-1)-2195 and from the National Science Foundation under Grant 74-09853ATM.

### REFERENCES

- Bunting, A. H., Dennet, M. D., Elston, J., and Milford, J. R. (1976). Rainfall trends in the West African Sahel. *Q.J.R. Meteorol. Soc.*, **102**, 59–64.
- Cressman, G. P. (1959). An operational objective analysis system. *Mon. Weather Rev.*, **87**, 367–374.
- Dubief, J. (1959). *Le Climat du Sahara*. Univ. Inst. Rech. Sahariennes, Mem. (hors sér.), Alger, 312 pp.
- Dubief, J. (1963). *Le Climat du Sahara*. Univ. Inst. Rech. Sahariennes, Mem. (hors sér.), Alger, 272 pp.
- Dubief, J. (1979). *Review of the North African Climate with Particular Emphasis on the Production of Eolian Dust in the Sahel Zone and in the Sahara*. In this report.
- Findlater, J. (1969a). A major low-level air current near the Indian Ocean during the northern summer. *Q.J.R. Meteorol. Soc.*, **95**, 362–380.
- Findlater, J. (1969b). Interhemispheric transport of air in the lower troposphere over the western Indian Ocean. *Q.J.R. Meteorol. Soc.*, **95**, 400–403.
- Findlater, J. (1972). Aerial explorations of the low-level cross-equatorial current over eastern Africa. *Q.J.R. Meteorol. Soc.*, **98**, 274–289.
- Flohn, H. (1965). Studies on the Meteorology off Tropical Africa. *Bonner Meteorol. Abh.*, **5**, 57 pp.
- Flohn, H., Henning, D., and Korff, H. C. (1965). Studies on the Water-vapour Transport over Northern Africa. *Bonner Meteorol. Abh.*, **6**, 36 pp.
- Gillette, D. A. (1979). *Environmental Factors Affecting Dust Emission by Wind Erosion*. In this report.
- Griffiths, J. F. (1972). Climates of Africa. *World Survey of Climatol.*, **10**, Elsevier, Amsterdam, 604 pp.
- Griffiths, J. F., and Soliman, K. H. (1972). Climates of Africa, Chapter 3. *World Survey of Climatol.*, **10**, 75–131, Elsevier, Amsterdam.

- Kalu, A. E. (1979). *The African Dust Plume: Its Characteristics and Propagation Across West Africa in Winter*. In this report.
- Kendrew, W. G. (1961). *The Climates of the Continents*. Oxford, 5th ed., 608 pp.
- Kidson, J. W. (1977). African rainfall and its relation to the upper air circulation. *Q.J.R. Meteorol. Soc.*, **103**, 441-456.
- Maley, J. (1976). Essais sur le rôle de la zone tropicale dans les changements climatiques; l'exemple africain. *C.R. Acad. Sci. Paris*, **283**, 337-340.
- Munitalp Foundation. (1960). *Tropical Meteorology in Africa*. Nairobi.
- Newell, R. E., Kidson, J. W., Vincent, D. G., and Boer, G. J. (1972). *The General Circulation of the Tropical Atmosphere*, Vol. 1, MIT-Press, Cambridge, Mass., 258 pp.
- Newell, R. E., Kidson, J. W., Vincent, D. G., and Boer, G. J. (1974). *The General Circulation of the Tropical Atmosphere*, Vol. 2. MIT-Press, Cambridge, Mass., 371 pp.
- Newell, R. E. (1973). Climate and the Galapagos Islands. *Nature*, **245**, 91-92.
- Parkin, D. W., and Shackleton, N. J. (1973). Trade wind and temperature correlations down a deep-sea core off the Saharan coast. *Nature*, **245**, 455-457.
- Peixoto, J. P. (1973). Atmospheric Vapour Flux Computations for Hydrological Purposes. *WMO/IHD Rep.*, **20**, WMO-357, 100 pp.
- Peixoto, J. P., and Obasi, G. O. P. (1965). Humidity Conditions over Africa during the IGY. *Sci. Rep.*, **7**, Planetary Circulations Project, MIT-Press, Cambridge, Mass., 143 pp.
- Prospero, J. M. (1979). *Monitoring Saharan Aerosol Transport by Means of Atmosphere Turbidity Measurements*. In this report.
- Prospero, J. M., and Carlson, T. N. (1972). Vertical and areal distribution of Saharan dust over the western equatorial North Atlantic Ocean. *J. Geophys. Res.*, **77**, 5255-5265.
- Rapp, A. (1974). A Review of Desertization in Africa - Water, Vegetation, and Man. *Secr. Int. Ecology*, Rep. 1, Stockholm, Sweden, 77 pp.
- Sircoulon, J. (1974). Les Données Climatiques et Hydrologiques de la Sècheresse en Afrique de l'ouest Sahélienne. *Secr. Int. Ecology*, Rep., 2, Stockholm, Sweden, 43 pp.
- Street, F. A., and Grove, A. T. (1976). Environmental and climatic implications of late quaternary lake-level fluctuations in Africa. *Nature*, **261**, 385-389.
- Struning, J. O., and Flohn, H. (1969). Investigations on the Atmospheric Circulation above Africa. *Bonner Meteorol. Abh.*, **10**, 55 pp.
- Tanaka, M., Weare, B. W., Navato, A. R., and Newell, R. E. (1975). Recent African rainfall patterns. *Nature*, **255**, 201-203.
- Thompson, B. W. (1965). *Climate of Africa*. Oxford Univ. Press, Nairobi, London, New York, 132 pp.
- Turekian, K. K. (1968). *Oceans*. Prentice-Hall, New York, 120 pp.
- Winstanley, D. (1973). Recent rainfall trends in Africa, the Middle East and India. *Nature*, **243**, 464-465.

